Crimson Publishers
Wings to the Research

Review Article

Selective Analysis of a High-Strength Steel Shielded Metal Arc Weld Metal Database

Krishna Sampath*

Santa Clara, CA, USA

ISSN: 2578-0255

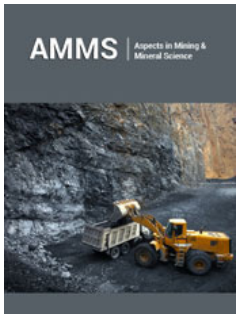

***Corresponding author:** Krishna Sampath, Santa Clara, CA, USA

Submission: August 14, 2024
Published: October 28, 2024

Volume 12 - Issue 4

How to cite this article: Krishna Sampath*. Selective Analysis of a High-Strength Steel Shielded Metal Arc Weld Metal Database. Aspects Min Miner Sci. 12(4). AMMS. 000795. 2024.
DOI: 10.31031/AMMS.2024.12.000795

Abstract

The current effort performed a novel, two-stage selective analysis of a large, Shielded Metal Arc (SMA) Weld Metal (WM) database posted online at ResearchGate by Dr. Glyn M Evans [1] together with the previously published analysis [2] using Constraints-Based Modeling (CBM), an Artificial Neural Network (ANN) offered by Japan Welding Engineering Society (JWES) at its web-site [3] and a machine learning algorithm that provided a New A_{r3} equation [4] as appropriate and effective tools to organize and analyze Evans's database in gaining valuable insights on welding electrode development and/or evaluation:

a.The first-stage selective analysis of TiBAlN series of WMs with N content below 85ppm (0.0085wt-%) used two metallurgical criteria involving CBM, New A_{r3} equation and JWES-ANN tool; and

b.The second-stage selective analysis used the results of the first-stage selective analysis and identified 61 WMs belonging to different Fe-C-Mn systems with N content below 100ppm (0.0010wt-%) to reaffirm that control of selected characteristics is essential to obtain high-performance WM microstructures.

Keywords: Yield strength; Pressure vessels; Machine; Temperature; Strength; Metal arc

Introduction

The two-stage selective analysis allowed a strong metallurgical basis involving chemical composition-processing-microstructure development and mechanical properties for developing and/or evaluating high-performance welding electrodes for joining High Strength Steels (HSSs). In particular, the intent was to meet the requirements for demand-critical applications such as structures in earthquake-prone locations [5], pipelines for cold climate applications [6], submarines and aircraft carriers that fulfill mandatory explosion bulge test requirements [7,8], pressure vessels, etc. Such demand-critical applications often require significant spread between Yield Strength (YS) and Ultimate Tensile Strength (UTS) of both base metals and relevant WMs.

SMA WM Database

In May 2015, Dr. Glyn M. Evans posted online a large, SMA WM database in ResearchGate [1]. This database contains over 900 compositions along with their respective WM tensile properties that include Yield Strength (YS), Ultimate Tensile Strength (UTS), Percent Elongation (%El) and Percent Reduction in Area (%RA) besides Charpy V-Notch (CVN) impact properties that include test temperatures T_{28J}/°C and T_{100J}/°C for achieving 28J and 100J impact energy, respectively. This database listed altogether 16 elements-C, Si, Mn, P, S, Cu, Ni, Cr and Mo in wt-%, and Nb (Cb), V, Ti, B, Al, N and O in ppm -of WM compositions and were derived from the book "Metallurgy of Basic Weld Metal," by G M Evans & N Bailey [5]. Commonly, C, Si, Mn,

Cu, Ni, Cr, Mo, Nb (Cb) and V are known as principal alloy additions in iron while Ti, B, Al, N, and O are called micro-alloying additions.

The individual chemical compositions of WMs in the SMA database varied over a wide range. Table 1 shows the high, low and range of individual elements in WM chemical composition in the SMA database. It is instructive to recognize that at about 0.12wt-% C, the morphology of martensite changes from needles to plates [9,10], and this morphological change in WM microstructure has adverse effects on both impact (fracture) toughness and Hydrogen-Induced Cracking (HIC) sensitivity. Controlling the C content below 0.10wt-% in WM is considered extremely desirable in achieving an exceptional combination of high strength and low-temperature impact (fracture) toughness.

Table 1: Low, high and range of chemical composition of individual elements (in wt-%) in Evans's SMAW database [1,2].

	C	Si	Mn	P	S	Cu	Ni	Cr	Mo	Nb	V	Ti	B	Al	N	O
High	0.152	1.11	2.1	0.04	0.046	2.04	5.48	3.5	1.16	0.098	0.2873	0.077	0.02	0.068	0.027	0.154
Low	0.035	0.001	0.23	0.003	0.003	0.02	0.03	0.026	0.005	0.0003	0.0003	0.0001	0.0001	0.0001	0.0035	0.022
Range	0.117	1.109	1.87	0.037	0.043	2.02	5.45	3.474	1.155	0.0977	0.287	0.0769	0.0199	0.068	0.0235	0.132

Availability of Evans's database involving a wide variety of Fe-C-Mn SMA WM compositions is an extremely valuable and rare gift to the welding community as it provides ready access to a wealth of data. All of these experimental SMAW electrodes belonged to the "basic" type. The test deposits were produced using standardized weld procedures, at Oerlikon Welding Limited, Zurich, Switzerland according to ISO 2560, at a nominal 1kJ/mm (about 25kJ/in.) heat input, 200 °C interpass temperature and 20mm plate thickness, by a single master welder. Figure 1 shows a typical macrograph of a test weld [11], the CVN being centrally located as shown by the vertical red line. The WM compositions in Evans's database belonged to 74 types of Fe-C-Mn alloy systems. A few of these 74 types, particularly involving TiB/CB/TiBN; ACuTi/Aplus; AoPlus/ANiTi and AlN/AlO/Al/AlTi showed identical chemical composition, tensile properties including YS, UTS, %El and %RA besides T_{28J}/°C and T_{100J}/°C temperatures, despite being designated as belonging to different sets of alloy systems.

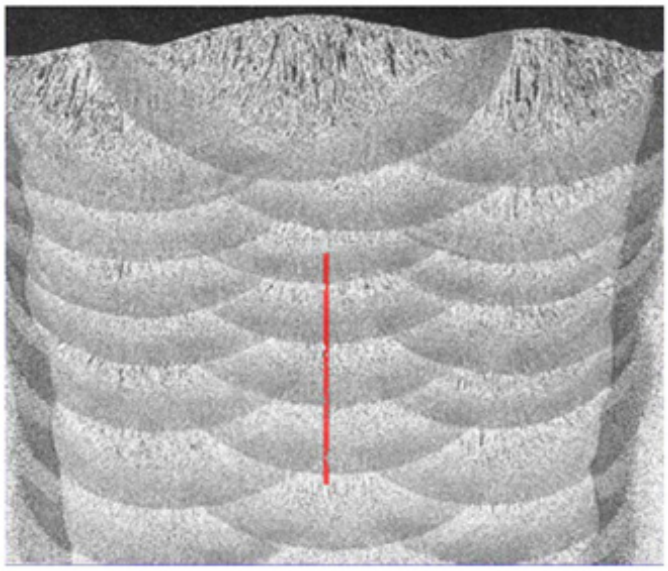

Figure 1: Cross-section of a typical test weldment with three beads per layer [11].

Selective Analysis

Previous analysis [2] of Evans's database enlisted two metallurgical criteria to control calculated austenite Transformation Temperatures (T_S) such as A_{r3m}, B_S or M_S besides C content below 0.10wt-%, Yurioka's [12] Carbon Equivalent Number (CEN) while balancing Ti, B, Al, N, O additions for producing desired high-performance WM microstructures that meet or exceed minimum tensile and CVN impact toughness property requirements for joining HSS. Yurioka's CEN is commonly used to evaluate the weldability of a variety of structural and pressure vessel steels, particularly, to assess the need and level of preheat to overcome HIC during fusion welding. With application of CBM, Yurioka's CEN is also used to identify WMs that overmatch WM tensile strength relative to base metal tensile strength thus ensuring a higher joint efficiency while complying with chemical composition requirements of relevant welding electrode specifications [13-16]. The second criterion is meant to simultaneously use both JWES-ANN tool [3] in balancing Ti, B, Al, N, O additions and New A_{r3} equation [4] for further lowering the actual T_S temperature to obtain high-performance Acicular Ferrite (AF) microstructures in WM.

These Calculated Metallurgical Characteristics (CMCs) provide near-accurate (but not exact) valuations of various T_S temperatures [17,18]. In particular, the CMCs of most WMs in Evans's database showed a progressive decrease in calculated values of various T_S temperatures, with $A_{r3m}>B_S>M_S$. When WMs show a progressive decrease in the calculated T_S temperatures as in $A_{r3m}>B_s>M_S$, austenite decomposition would result in predominantly diffusional transformation products instead of athermal transformation products, depending on the actual weld cooling rate. Prior analysis [2] had shown that control of C content below 0.10wt-%, values of Yurioka's CEN and actual or calculated austenite Transformation-Start (T_S) temperature is critical for developing, identifying and/or evaluating the occurrence of high-performance WM microstructures. Secondly, the "JWES-ANN tool" is extremely valuable in manipulating the addition of 16 elements-C, Si, Mn, P, S, Cu, Ni, Cr and Mo in wt-%, and Nb (Cb), V, Ti, B, Al, N and O in ppm, each within a restricted range [3].

This manipulation allows one to estimate and/or lower the T_{28J}/°C test temperature much below -60 °C for achieving 28J impact energy during Charpy V-Notch (CVN) impact testing. Bhadeshia et al. [19] have described in detail the development of an ANN technique within a Bayesian framework using CVN toughness data on SMAW

and Submerged Arc Welded (SAW) samples. All of the data used in this ANN technique were based on experiments conducted at the ESAB Central Research Laboratories, Sweden. However, unlike the JWES-ANN tool, this research article by Bhadeshia et al. [19] did not provide a template to estimate the CVN test temperature for achieving either T_{28J}/°C or T_{100J}/°C. Subsequent application of machine learning to a set of datasets [4] including Evans's database provided the following equation for calculating the New A_{r3} temperature based on chemical composition of 14 elements (C, Si, Mn, Cu, Ni, Cr, Mo, Nb (Cb), V, Ti, B, Al, N, and O, except P and S) within specified ranges and weld cooling rate (in °C/s).

$$New\,A_{r3}(°C) = 906.49 - 2.78(CR) - 439.3(C) + 34.17(Si) - 36.7(Mn) - 8.5(Cu) - 51.2(Ni) - 27.08(Cr) - 63.48(Mo) - 1765.95(Nb) - 520.29(V) - 2401.12(Ti) - 1784.44(B) + 21.89(Al) + 5300.15(N) - 420.96(O) + 297.07(C^2) - 16.4(Mn^2) + 11668.54(Nb^2) + 458.21(\sqrt{Ti}) - 1142.45(\sqrt{N}) + 298.91(\sqrt{O}) \quad \text{(Equation 1)}$$

where CR refers to cooling rate in °C/s. The adjusted r^2 of this equation is 0.9087. The intercept value of this New A_{r3} equation at 906.49 °C which is close to 910 °C that corresponds to the A_{e3} (equilibrium austenite-ferrite transformation) temperature for pure iron. Equation 1 shows that besides N content, C, Nb, V, Ti and B additions can substantially lower the calculated values of New A_{r3} temperature, more so at a higher weld cooling rate, requiring proper control over the above six elemental additions. Readers could also consider including the calculated New A_{r3} temperature to the set of CMCs. The above equation for New A_{r3} temperature is particularly relevant for the formation of high-performance AF microstructures in WM. Commonly, nucleation of AF is facilitated at near-good lattice matching across an inclusion surface and the resultant microstructural constituent. As is well known, Al, Ti, Si and Mn are strong deoxidizers. When the Al content is typically below 160ppm (0.016wt-%) together with modest amounts of Ti and B additions, Al tends to form Al_2O_3 inclusions with an amorphous TiO layer [20-22]. Presence of B enables the formation of an amorphous TiO layer on the surface of Al_2O_3 inclusions. The B absorption in the amorphous phase has been found to enhance intra-granular nucleation of ferrite.

Prior research by Takada et al. [23] had reported that in WM samples containing low (50ppm or 0.005wt-%) and medium (150ppm or 0.015wt-%) Al contents, the nucleation of AF occurred on the surface of inclusions. However, occurrence of AF was observed to be scarce in WM samples containing a higher (390ppm or 0.039wt-%) Al content. Takada et al. [23] had also reported that grain boundary ferrite formed only in a WM sample with a low Al content (50ppm or 0.005wt-%) but scarcely formed in WM samples containing medium (150ppm or 0.015wt-%) and high (390ppm or 0.039wt-%) Al contents. Furthermore, Ito et al. [24] had reported that it is possible to maximize the content of intra-granularly nucleated AF by increasing intragranular nucleation sites with the addition of about 250ppm (0.025wt-%) O in WM while maintaining or exceeding a critical weld cooling rate. Interestingly, Takada et al. [23] had reported that grain boundary ferrite formed at a temperature just below 660 °C, prior to the onset of intra-granularly nucleated AF at a temperature just below 630 °C. The above metallurgical understanding of the effects of certain micro-alloying elements on intra-granularly nucleated AF allows one to aim at an Al content below 100ppm (0.01wt-%), a N content much lower than 100ppm (0.01wt-%), O content at about 250ppm (0.025wt-%) with marginal additions of Ti and B in about 10:1 ratio and about 700 °C±30 °C as a desirable target range for the austenite-to-ferrite T_S temperature in Fe-C-Mn WMs. Furthermore, based on the work of Takada et al. [23], one might recognize that grain boundary ferrite might form when the Al content is extremely low, much below 50ppm (0.005wt-%).

Result & Discussion

Table 2 shows the chemical composition of the first set of 8 SMA WMs belonging to the TiBAlN series, with normal N content at less than 85ppm or 0.0085wt-% [25-27] that produced a predominantly AF microstructure in WMs. Subsequent dilatometric evaluation studied the transformation temperatures during continuous cooling from 800 °C to 500 °C (i.e., $\Delta t_{8/5}$). Test specimens were machined to form hollow cylinders with the following dimensions: 10mm long×5mm outside diameter with 1mm wall thickness. The axis of the test specimen was maintained parallel to the original welding direction. The specimens were subjected to the following controlled thermal cycle: austenitization at 1250 °C for two minutes followed by continuous cooling at a typical (weld) cooling rate of 13 °C/s over $\Delta t_{8/5}$. The study determined the T_S and T_F temperatures of the above 6 welds. The T_S and T_F temperatures of a seventh weld W[1] were also obtained separately, at a typical (weld) cooling rate of 13 °C/s.

Table 2: Chemical composition (in wt-%) of eight WMs with controlled Ti-B-Al-N-O additions [25-27].

Weld ID	C	Si	Mn	P	S	Ti	B	Al	N	O	(Ti+B+Al+N+O)
O	0.074	0.25	1.40	0.007	0.008	0.0001	0.0001	0.0006	0.0079	0.0475	0.0562
W	0.077	0.27	1.46	0.007	0.008	0.0028	0.0003	0.0005	0.0081	0.0459	0.0576
X	0.069	0.45	1.47	0.006	0.005	0.041	0.0002	0.0001	0.0077	0.0282	0.0772

[1]The T_S and T_F temperatures of weld W were obtained in a private communication from Dr. G M Evans.

Y	0.07	0.45	1.57	0.01	0.006	0.039	0.0039	0.0013	0.0083	0.0308	0.0833
Z	0.072	0.49	1.56	0.01	0.007	0.042	0.0048	0.016	0.0067	0.0438	0.1133
T	0.064	0.4	1.49	0.005	0.007	0.0005	0.0195	0.0005	0.0085	0.0503	0.0793
U	0.073	0.4	1.52	0.011	0.006	0.039	0.0158	0.0005	0.0084	0.029	0.0927
V	0.078	0.6	1.44	0.007	0.006	0.054	0.0056	0.058	0.0041	0.044	0.1657
Average	0.072	0.41	1.49	0.008	0.007	0.0273	0.0063	0.0097	0.0075	0.0399	0.0907
High	0.078	0.6	1.57	0.011	0.008	0.054	0.0195	0.058	0.0085	0.0503	0.1657
Low	0.064	0.25	1.40	0.005	0.005	0.0001	0.0001	0.0001	0.0041	0.0282	0.0562
Range	0.014	0.35	0.17	0.006	0.003	0.0539	0.0194	0.0579	0.0044	0.0221	0.1095

Importantly, the dilatometric analysis of the SMA WMs belonging to the TiBAlN series with N content below 85ppm (0.0085wt-%) formed the cornerstone for correlating WM chemical composition and weld mechanical properties with a need to "balance" Ti-B-Al-N-O content that could promote a lower T_S temperature, a narrower (T_S-T_F) temperature range leading to a "cloudburst" of austenite to AF transformation. Dilatometric results illustrated in (Table 3) revealed weld Y had the lowest 150 °C difference between T_S and T_F, while weld Z had a 160 °C difference between T_S and T_F, followed by weld U with a 169 °C difference between T_S and T_F, all three WMs had low N content below 85ppm (0.0085wt-%). In weld Y, the Ti-B-Al-N-O addition at 833ppm (0.0833wt-%) appeared to provide a "near" balance that was perhaps quite effective in producing a "cloudburst" of solid-state phase transformation that likely aided the formation of refined AF microstructure over a narrow (T_S-T_F) temperature range. In weld Z, the total Ti-B-Al-N-O content at 1133ppm (0.1133wt-%) appeared over 40% excessive compared to weld Y. As shown in Table 3, the first stage analysis of Evans's TiBAlN series with low N content (below 85ppm or 0.0085wt-%) based on dilatometry [25-27] showed that a nearly "balanced" Ti-B-Al-N-O micro-alloying addition in weld Y achieved: 1) a low T_S temperature at 710 °C; 2) a narrower start-to-finish (T_S-T_F) temperature range at 150 °C; 3) actual T_{28J}/°C test temperature at -114 °C; and 4) a 48MPa spread between YS and UTS during ambient tensile testing of weld Y, with YS/UTS ratio at 0.92.

Table 3: Experimental results on transformation temperatures, tensile and CVN impact properties and of WMs with controlled Ti-B-Al-N-O additions [25-27].

Weld ID	Experimental Transformation Temperature (°C) at 13 °C/s			WM Tensile Properties					CVN Test Temperature (°C)	
	T_S	T_F	(T_S – T_F)	YS (MPa)	UTS (MPa)	YS/UTS	El(%)	RA(%)	T_{100J}/°C	T_{28J}/°C
O	762	554	208	445	528	0.84	28.2	78	-14	-42
W	764	568	196	471	544	0.87	25.2	77	-68	-88
X	760	568	192	504	577	0.87	25.8	79.8	-61	-77
Y	710	560	150	546	594	0.92	25.8	73	-84	-114
Z	710	550	160	610	640	0.95	27.2	73.4	-83	-100
T	---	---	---	478	561	0.85	22.2	73.6	-34	-75
U	700	531	169	517	586	0.88	22.5	77.7	-53	-80
V	680	507	173	668	732	0.91	20.3	69.7	-12	-46
High	764	568	208	668	732	0.95	28.2	79.8	-12	-42
Low	680	531	150	445	528	0.84	20.3	69.7	-84	-114
Range	84	37	58	223	204	0.11	7.9	10.1	72	72

The CMCs showed CEN of these 8 WMs ranged between 0.219 and 0.277, and a progressive decrease in calculated values of transformation temperatures of each WM, i.e., A_{r3m}>B_S>M_S [28]. The CMCs also report the calculated New A_{r3} temperature [28] that ranged between 703 °C and 757 °C. Table 4 shows the calculated New A_{r3} temperature (in °C) of 8 WMs at 13 °C/s weld cooling rate along with the dilatometric results of 7 WMs (except weld T). Except for welds V and X that showed a substantial difference between the calculated New A_{r3} temperature and actual T_S temperature determined using dilatometry, all other welds showed only a minor difference (less than 18 °C) between the calculated New A_{r3} temperature and actual T_S temperature. Furthermore, Table 4 clearly illustrates the benefit of "balancing" Ti, B, Al and O additions with three types of controlled Ti-B-Al-N-O additions including N corresponding to welds W (576ppm), Z (1133ppm) and Y (833ppm), and the role of JWES-ANN tool [3] in predicting this effect in substantially lowering the T_{28J}/°C of various WMs with a predominantly AF microstructure.

Table 4: Predicted CVN test temperature of TiBAlN series WMs with three types of controlled Ti–B–Al–N–O additions.

Weld ID	T_S Temperature (°C) Determined by Dilatometry	Calculated New A_{r3} Temperature (°C) at 13 °C/s	YS/UTS of Original Weld	Experimental CVN Test Temperature (T_{28J}/°C)	JWES-ANN Predicted CVN Test Temperature (T_{28J}/°C)			
					Predicted Value for Original Weld	Predicted Value when Ti-B-Al-N-O Additions Balanced as in Weld W	Predicted Value when Ti-B-Al-N-O Additions Balanced as in Weld Z	Predicted Value when Ti-B-Al-N-O Additions Balanced as in Weld Y
O	762	750	0.84	-42	-49	-82	-82	-88
W	764	757	0.87	-88	-82	---	-85	-93
X	760	736	0.87	-77	-80	-88	-90	-96
Y	710	724	0.92	-114	-102	-87	-94	-
Z	710	727	0.95	-100	-94	-88	-	-103
T	---	722	0.85	-75	-77	-87	-87	-93
U	700	703	0.88	-80	-79	-84	-92	-99
V	680	728	0.91	-46	-47	-89	-95	-103
High	764	757	0.95	-42	-47	-82	-82	-88
Low	680	703	0.84	-114	-102	-89	-95	-103
Range	16	54	0.11	72	55	7	13	15

Compared to Ti–B–Al–N–O additions as in welds W and Z, the Ti-B-Al-N-O additions in weld Y contributed to the largest decrease in T_{28J}/°C of 7 welds. This behavior is attributed to either the actual T_S temperature determined using dilatometry and/or the calculated New A_{r3} temperature, with a lower T_S temperature requiring a lower amount of balanced Ti-B-Al-N-O additions. While the Ti-B-Al-N-O additions in welds W, Y and Z showed nearly a 10:1 ratio between Ti and B contents, both welds W and Z contained higher levels of O, in excess of 430ppm (0.043wt-%) compared to weld Y, and much higher than 250ppm (0.025wt-%) O recommended by Ito et al. [24]. The above selective consideration of the first set of TiBAlN series WMs with low N (85ppm or less) indicated that nearly "balanced" Ti-B-Al-N-O micro-alloying addition as in weld Y achieved: 1) A low T_S temperature at 710 °C; 2) A narrow (T_S-T_F) temperature at 150 °C; 3) C content below 0.10wt-%; 4) Yurioka's CEN below 0.300; 5) A nearly balanced Ti-B-Al-N-O content at 833ppm (0.0833wt-%); 6) Actual T_{28J}/°C of -114 °C, besides 7) YS/UTS ratio at 0.92.

In particular, a narrower (T_S-T_F) temperature range at 150 °C seemed to enable a "cloudburst" of solid-state phase transformation resulting in refined microstructural features. Inter alia, both a lower T_S temperature and a narrow (T_S-T_F) temperature range due to a "balanced" Ti-B-Al-N-O content ensured a WM with superior combination of high strength and exceptional CVN impact toughness. A low T_S temperature and a narrower (T_S-T_F) temperature range also appeared to promote a significant spread between YS and UTS during ambient tensile testing of WMs with YS/UTS ratio at or below 0.92 thereby providing a superior combination of excellent ductility and low-temperature impact toughness. Based on the first set of low N WMs from TiBAlN series, a second set of 61 WMs was selected from Evans's database [28] for further analysis. All these 61 WMs contained N lower than 100ppm (0.01wt-%) with YS/UTS ratio between 0.82 and 0.92, and T_{28J}/°C between -114 °C and -90 °C. These 61 WMs included weld Y from Evans's database with a predominantly AF microstructure in WM but didn't include weld Z, as the YS/UTS ratio of weld Z was higher than 0.92. Subsequently, a clustering analysis of these 61 WMs was performed to relate Ti-B-Al-N-O addition in achieving YS/UTS ratio between 0.84 and 0.92.

The second set of 61 low nitrogen WMs (including weld Y) had N content below 100ppm (0.010wt-%). These 61 WMs also showed a common progression of calculated T_S temperatures with A_{r3m}>B_S>M_S for each of these WMs. The YS of these 61 WMs ranged between 417MPa and 589MPa while UTS ranged between 498MPa and 65MPa. Readers could readily recognize that all 61 WMs had YS/UTS ratio between 0.82 and 0.92, revealing nearly balanced Ti-B-Al-N-O additions. The calculated New A_{r3} temperature (at 13 °C/s weld cooling rate) of these 61 WMs ranged between 646 °C and 820 °C [28]. Within the same type of Fe-C-Mn alloy system, WMs with a lower calculated New A_{r3} temperature most often showed a correspondingly higher WM UTS.

The C content of these 61 WMs ranged between 0.038wt-% and 0.094wt-% while Yurioka's CEN ranged between 0.153 and 0.271. The T_{28J}/°C ranged between -114 °C and -90 °C while T_{100J}/°C ranged between -85 °C and -60 °C. The T_{28J}/°C results were much lower than -60 °C used as a "benchmark" for achieving exceptional 28J absorbed energy with nearly balanced Ti-B-Al-N-O additions using the JWES-ANN tool. The total (Ti+B+Al+N+O) content of these 61 WMs belonging to a variety of alloy systems varied between a low of 327ppm (0.0327wt-%) and a high of 986ppm (0.0986wt-%). As illustrated in Figure 2, the clustering analysis of 61 WMs revealed that a balanced Ti-B-Al-N-O addition between 500ppm (0.05wt-%) and 600ppm (0.06wt-%) appeared preferable in achieving YS/UTS ratio between 0.84 and 0.92. Thirty-three of these 61 WMs [28] showed YS ranged between 417MPa and 58MPa while their UTS ranged between 498MPa and 650MPa. The YS/UTS ratio of these 33 WMs ranged between 0.84 and 0.92. The total (Ti+B+Al+N+O) content of these 33 WMs ranged between 501ppm (0.0501wt-%) and 593ppm (0.0593wt-%). The C content range continued to

stay between 0.038wt-% and 0.094wt-% as in 61 WMs, and the calculated New A_{r3} temperature also stayed between 646 °C and 820 °C as in 61 WMs while the CEN ranged between 0.153 and 0.263.

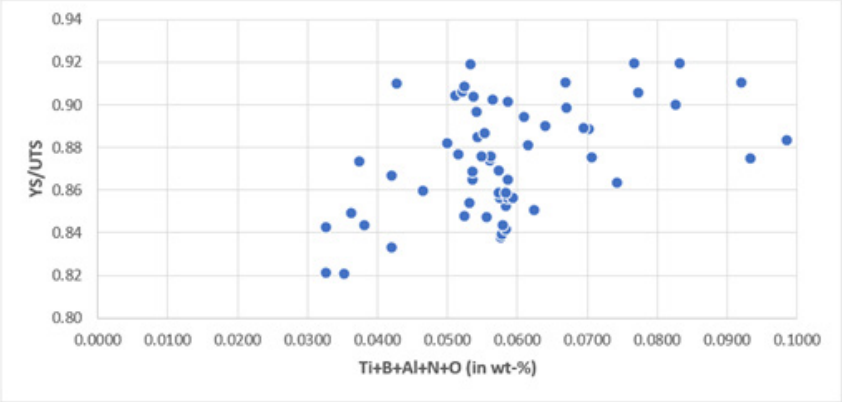

Figure 2: Clustered results show Ti-B-Al-N-O addition between 0.05wt-% and 0.06wt-% is preferable to achieve YS/UTS ratio between 0.84 and 0.92.

Each of these 33 WMs also showed a progressive decrease in calculated T_S temperature with $A_{r3m}>B_s>M_s$. The T_{28J}/°C values of these 33 WMs ranged between -114 °C and -90 °C, while T_{100J}/°C values ranged between -85 °C and -60 °C. Furthermore, as shown in Figure 3, application of the JWES-ANN tool to the average chemical composition of these 33 WMs with the calculated New A_{r3} temperature at 740 °C, CEN at 0.221 and total Ti-B-Al-N-O additions at 556ppm (0.0556wt-%) showed T_{28J}/°C below -95.0 °C, subject to experimental verification. Interestingly, as shown in left column of Figure 4, application of the JWES-ANN tool to the average chemical composition of 61 WMs with the calculated New A_{r3} temperature at 745 °C, CEN at 0.229 and total Ti-B-Al-N-O additions at 586ppm (0.0586wt-%) showed a T_{28J}/°C of -78.4 °C, subject to experimental verification. However, as shown in the right column of Figure 4, application of JWES-ANN tool showed that when a marginal reduction in total Ti-B-Al-N-O additions at 556ppm (0.0556wt-%) of the average of 33 WM compositions is substituted for Ti-B-Al-N-O content in the average chemical composition of 61 WMs at 586ppm (0.0586wt-%), the T_{28J}/°C is further reduced from -78.4 °C to -92.5 °C, subject to experimental verification.

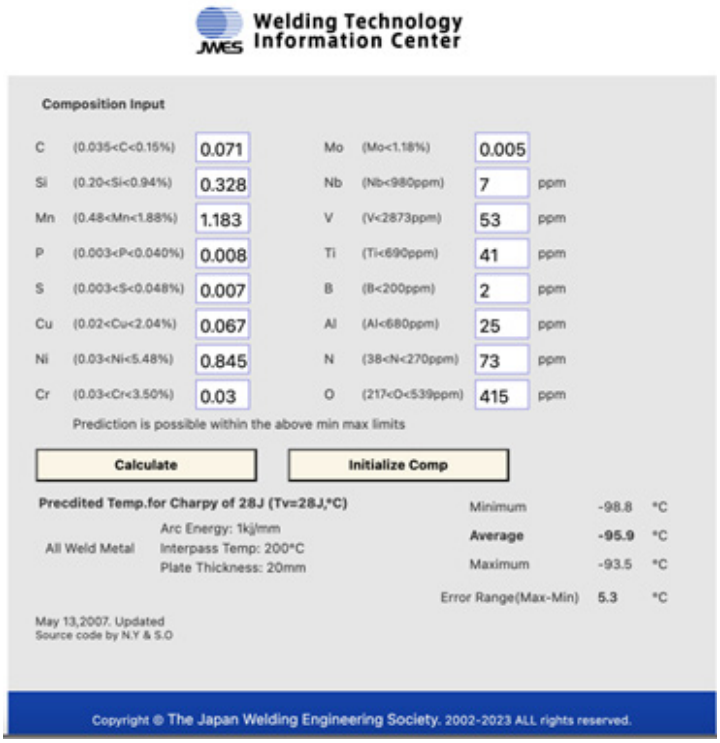

Figure 3: JWES-ANN prediction of T_{28J}/°C for the average composition of 33 WMs.

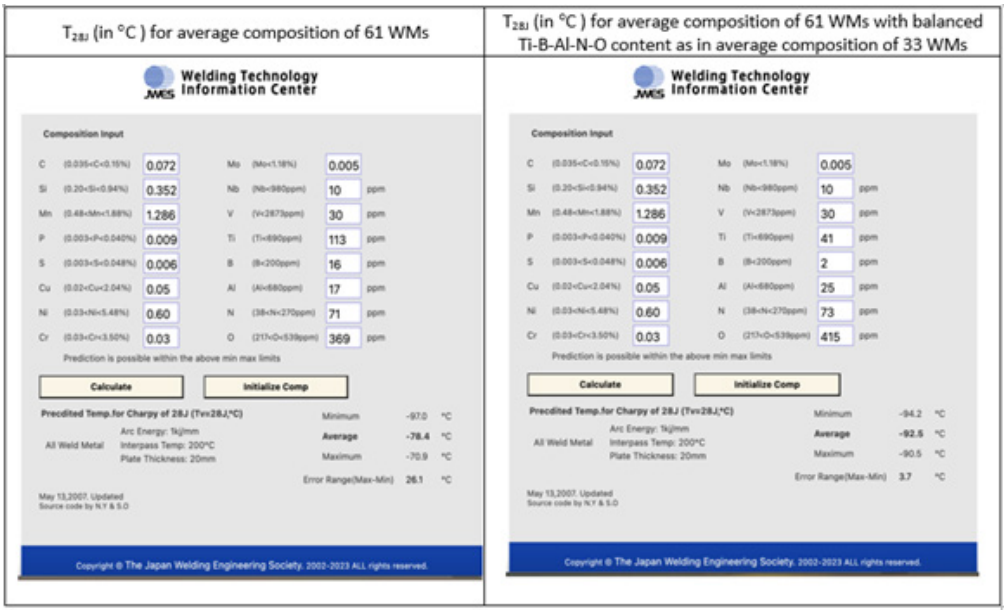

Figure 4: JWES-ANN prediction of T_{28J}/°C for the average composition of 61 WMs with "balanced" Ti-B-Al-N-O additions.

With the above change in Ti-B-Al-N-O content with Ti at 41ppm (0.0041wt-%), B at 2ppm (0.0002wt-%), Al at 25ppm (0.0025wt-%), N at 73ppm (0.0073wt-%), and O at 415ppm (0.041wt-%), the calculated New A_{r3} temperature marginally increased from 745 °C to 746 °C, while CEN reduced from 0.229 to 0.225. The "balanced" total Ti-B-Al-N-O content at 556ppm (0.0556wt-%) is somewhat similar to the total (Ti+B+Al+N+O) content of weld W at 576ppm (0.0576wt-%), with Ti at 28ppm (0.0028wt-%), B at 3ppm (0.0003wt-%), Al at 5ppm (0.0005wt-%), N at 81ppm (0.0081wt-%), and O at 459ppm (0.0459wt-%). It is further articulated that as the calculated New A_{r3} or actual T_S temperature is further lowered, one could further reduce the total content of Ti-B-Al-N-O additions, in particular O addition near 250ppm (0.0250wt-%) thereby enabling a narrow (T_S-T_F) temperature range and a lowering of YS/UTS ratio, subject to experimental verification. Based on the above examples, Equation 1 to calculate New A_{r3} temperature that embodies the effects of 14 major and minor alloy elements (in wt-%) besides weld cooling rate (in °C/s) appears extremely useful in achieving about 700 °C±30 °C temperature and is expected to further complement the JWES-ANN template for predicting a T_{28J}/°C lower than -80 °C. These two computational tools [3,4] can be used with minimal risk in the efficient development and/or evaluation of welding electrode compositions based on Fe-C-Mn system that would likely provide a predominantly AF microstructure in WM to meet or exceed the requirements for high-performance and demand-critical applications [5-7] and achieve YS/UTS ratio between 0.84 and 0.92.

Summary

A novel, two-stage selective analysis of Evans's database was performed to obtain a strong metallurgical basis for developing and/or evaluating high-performance welding electrodes for joining HSS in demand-critical applications. The first stage analysis of Evans's TiBAlN series with low N content (below 85ppm or 0.0085wt-%) showed that a nearly "balanced" Ti-B-Al-N-O micro-alloying addition in weld Y achieved: 1) A low T_S temperature at 710 °C; 2) A narrower start-to-finish (T_S-T_F) temperature range at 150 °C; 3) Actual T_{28J}/°C test temperature at -114 °C; and 4) A 48MPa spread between YS and UTS during ambient tensile testing of weld Y with YS/UTS ratio at 0.92.

The second stage analysis of Evans's database with low N content (below 100ppm or 0.010wt-%) revealed a total of 61 WMs with T_{28J}/°C test results between -114 °C and -90 °C with YS/UTS ratio between 0.84 and 0.92. A clustering analysis of these 61 WMs revealed that a total Ti-B-Al-N-O addition between 0.05wt-% and 0.06wt-% is expected to achieve a significant spread between YS and UTS of WM while simultaneously providing a superior combination of excellent ductility and low-temperature impact toughness. The choice or selection of consumable electrodes for fusion welding of HSSs can immensely benefit from the above detailed understanding of the relationships among actual chemical composition, T_S temperature and cooling rate to form desirable high-performance WM microstructures with exceptional combination of higher strength and superior low-temperature impact toughness.

When considering impact toughness, application of JWES-ANN tool [3] has shown that one could leverage T_{28J}/°C test temperatures for 28J impact toughness values, subject to CVN impact testing over a broad temperature range. The 33 selected WMs [28] from Evans's database belonging to a variety of alloy systems showed a decreasing CVN impact test temperature for 28J WM toughness, with T_{28J}/°C CVN test temperature between -114 °C and -90 °C. The experimentally determined tensile strength of these 33 WMs ranged between 498MPa (72.2ksi) and 650MPa (94.3ksi). Coincidentally, a combination of C content of less than 0.10wt-%, Yurioka's CEN less than 0.300 (or corresponding to about 700MPa or 101ksi WM

tensile strength) and a calculated New A_{r3} temperature [4] at 700 °C ± 30 °C with a balanced Ti-B-Al-N-O addition between 0.05wt-% and 0.06wt-% appeared to provide a benchmark for improving CVN impact toughness or lowering the ductile-to-brittle CVN impact transition temperature. The above findings are also consistent with previously published recommendations on how to select welding electrodes for joining HSSs [29].

While the application of CBM to WM compositions doesn't allow one to study and analyze the interactive effects of minor alloy elements like Ti, B, Al, N and O in various Fe-C-Mn alloy systems without additional supporting microstructural analysis of WM [10], it appeared that Ti-B-Al-N-O additions likely provided a target for electrode "aim" compositions with "balanced" Ti-B-Al-N-O content between 0.05wt-% and 0.06wt-% to: 1) Achieve effective deoxidation; 2) Form complex inclusions; 3) Distribute them to enable development of a "cloudburst" of fracture-resistant and refined WM microstructure; 4) Promote significant spread between WM YS and UTS; and 5) Achieve a low T_{28J}/°C impact test temperature for 28J CVN impact toughness. Without the help of CBM, calculated New A_{r3} temperature and JWES-ANN tool, it might be virtually impossible to analyze a large SMA WM database containing over 900 WM chemical compositions and mechanical property data and develop the above set of valuable insights on efficient development and/or evaluation of welding electrode compositions based on various types of Fe-C-Mn system.

References

1. Evans GM (2015) Database-weld metal composition and properties.
2. Sampath K (2021) Analysis of a high-strength steel SMAW database. Welding Journal 100(10): 410-420.
3. Online calculator for the Charpy impact transition temperature that satisfies the 28J.
4. Varadarajan R, Sampath K (2023) Application of machine learning to regression analysis of a large SMA weld metal database. Welding Journal 102(3): 31-52.
5. Evans GM, Bailey N (1999) Metallurgy of basic weld metal. Abington Publishing, Abington, UK
6. Miami FL (2016) Structural welding code-Seismic supplement. American Welding Society. AWS D1.8/D1.8M.
7. Ohaeri EG, Szpunar JA (2022) An overview on pipeline steel development for cold climate applications. Journal of Pipeline Science and Engineering 2(1): 1-17.
8. Schank JF, Cesse IP, Lacroix FW, Murphy RE, Arena MV, et al. (2011) Learning from Experience Volume II: Lessons from the U S Navy's Ohio, Seawolf, and Virginia submarine programs. RAND Corporation p. 155.
9. Sugiyama M, Sawa G, Hata K, Maruyama N (2019) Heterogeneous microstructure of low-carbon lath martensite with continuous yielding behavior in Fe-C-Mn alloys. IOP Conf Ser: Materials Science and Engineering p. 580.
10. Jorge JCF, De Souza LFG, Mendes MC, Bott IS, Araúj LS, et al. (2021) Microstructure characterization and its relationship with impact toughness of C-Mn and high strength low alloy steel weld metals-A review. Journal of Materials Research and Technology 10: 471-501.
11. Evans GM (2018) A reassessment of the predictive charpy-V toughness of the manganese-nickel weld metal combination. IIW Doc II-C-546-18.
12. Yurioka N, Suzuki H, Ohshita S, Saito S (1983). Determination of necessary preheating temperature in steel welding. Welding Journal 62(6): 147s-153s.
13. (1994) Military specification: Electrodes and rods- welding, bare, solid, or alloy cored; and fluxes, low alloy steel, MIL-E-23765/2E.
14. Specification for carbon steel electrodes for shielded metal arc welding. American Welding Society (AWS), Florida, USA, AWS A5.1/A5.1M:2012.
15. Specification for low-alloy steel electrodes for shielded metal arc welding. American Welding Society (AWS), Florida, USA, AWS A5.5/A5.5M:2022.
16. Specification for low-alloy steel electrodes and rods for gas shielded arc welding. American Welding Society (AWS), Florida, USA, AWS A5.28/A5.28M:2022.
17. Ouchi C, Sampei T, Kozasu I (1982) The effect of hot rolling condition and chemical composition on the onset temperature of γ-α transformation after hot rolling. Transactions of the Iron and Steel Institute of Japan 22(3): 214-222.
18. Steven W, Haynes AG (1956) The temperature of formation of martensite and bainite in low-alloy steels. Journal of the Iron and Steel Institute 183(8): 349-359.
19. Bhadeshia HKDH, MacKay DJC, Svensson LE (1995) Impact toughness of C-Mn steel arc welds-Bayesian neural network analysis. Materials Science and Technology 11(10): 1046-1051.
20. Fox AG, Evans GM (2013) A comparative study of the non-metallic inclusions in C-Mn steel weld metals containing titanium or aluminium. Trends in Welding Research. In: DebRoy T, David SA, DuPont JN, Koseki T, Bhadeshia HK (Eds.), ASM International, pp. 623-630.
21. Loder D, Michelic SK, Bernhard C (2017) Acicular ferrite formation and its influencing factors-A review. J Mater Sci Res 6(1): 24-43.
22. Yamada T, Terasaki H, Komizo Y (2009) Relation between inclusion surface and acicular ferrite in low carbon low alloy steel weld. ISIJ Int 49(7): 1059-1062.
23. Takada A, Terasaki H, Komizo Y (2013) Effect of aluminium content on acicular ferrite formation in low carbon steel weld metals. Sci Technol Weld Joining 18(2): 91-97.
24. Ito Y, Nakanishi M, Komizo Y (1982) Effects of oxygen on low carbon steel weld metal. Metal Construction 14(9): 472-478.
25. Ilman MN, Cochrane RC, Evans GM (2012) Effect of nitrogen and boron on the development of acicular ferrite in reheated C-Mn-Ti steel weld metals. Welding in the World 56: 41-50.
26. Ilman MN, Cochrane RC, Evans GM (2014) Effect of titanium and nitrogen on the transformation characteristics of acicular ferrite in reheated C-Mn steel weld metals. Welding in the World 58: 1-10.
27. Ilman MN, Cochrane RC, Evans GM (2015) The development of acicular ferrite in reheated Ti-B-Al-N-type steel weld metals containing various levels of aluminium and nitrogen. Welding in the World 59: 565-575.
28. Sampath K (2024) Selected SMA WMs from Evans Database.
29. Sampath K (2007) How to choose electrodes for joining high-strength steels. Welding Journal 86(07): 26-28.